CHARACTERIZATION, MODELING, AND SIMULATION OF $In_{0.12}Al_{0.88}N/GaN$ HEMTs

*Marián Molnár[1,2], Gesualdo Donnarumma[1], Vassil Palankovski[1], Ján Kuzmík[1,3], Daniel Donoval[2], Jaroslav Kováč[2], and Siegfried Selberherr**

[1]Advanced Materials and Device Analysis group at nst. for Microelectronics, Technische Universität Wien, Austria; [2]Inst. of Electronics and Photonics, Slovak University of Technology, Bratislava, Slovakia; [3]Inst. of Electrical Engineering, Slovak Academy of Sciences, Bratislava, Slovakia

E-mail: marian.molnar@stuba.sk, molnar@iue.tuwien.ac.at

Received 04 May 2012; accepted 15 May 2012.

1. Introduction

GaN-based High Electron Mobility Transistors (HEMTs) attract strong attention due to their material relevant properties, such as wide bandgap, high carrier saturation velocity, thermal conductivity, and high breakdown field, which are required for high-temperature, high-power, and high-speed applications [1-3]. In this work, we study InAlN/GaN HEMT structures both experimentally and by means of two-dimensional device simulation with Minimos-NT [4,5]. Next to the DC device characteristics, special emphasize is given to the HEMT off-state breakdown behavior. The device structure and fabrication process are presented in Section 2, physics-based modeling and device simulation are described in Section 3, while experimental results and discussion are presented in Section 4.

2. Device structure

The investigated HEMT structure is schematically sketched in Fig.1. The InAlN/GaN heterostructure was grown by metal-organic vapor phase epitaxy (MOVPE) [6]. A 300nm thick AlN layer was grown on a 6H-SiC substrate followed by a 2.5µm GaN buffer layer with 1nm AlN spacer and 7nm $In_{0.12}Al_{0.88}N$ barrier on top. All layers are non-intentionally doped. The device width is 400µm. The drain and source Ohmic contacts were prepared by evaporation of a Ti/Al/Ni/Au metal stack with subsequent rapid thermal annealing, while the Schottky gate contact was formed using Ni/Au metalization [6]. The gate length is 1.6µm, and the gate-to-drain and gate-to-source distances are 4.8µm and 1.6µm, respectively.

3. Physics-based modeling

Two-dimensional hydrodynamic simulation was performed with Minimos-NT. The hydrodynamic transport model [7] includes the Poisson, electrons and holes current continuity, and the energy balance equations, which are solved self-consistently. These equations rely on a well-calibrated set of material-specific model parameters, which depend on temperature, carrier energy, etc. [8,9]. For example, Fig.2 shows the dependence of the bandgap energy E_g^{InAlN} in $In_xAl_{1-x}N$ at room temperature on In content x. In our model we consider a quadratic interpolation $E_g^{\mathrm{InAlN}} = (1-x)\cdot E_g^{\mathrm{AlN}} + x\cdot E_g^{\mathrm{InN}} + x\cdot(1-x)\cdot C_g$ between the bandgap energies of AlN $E_g^{\mathrm{AlN}} = 6.12\mathrm{eV}$ and InN $E_g^{\mathrm{InN}} = 0.64\mathrm{eV}$, respectively. As seen in Fig.2, the best agreement to experimental values [10-15] is obtained by using a bowing factor $C_g = -6\mathrm{eV}$, which results in $E_g^{\mathrm{InAlN}} = 4.84\mathrm{eV}$ for x=0.12. Because of the invariant total

polarization charge, the 1nm AlN spacer layer and the 7nm InAlN are replaced by 8nm thick InAlN layer [16]. Due to the divergence of the polarization fields at the InAlN/GaN heterointerface, a two-dimensional electron gas (2DEG) is formed in the quantum well. The 2DEG density (n_{2DEG}) depends on the In content, where for $In_{0.12}Al_{0.88}N$ we calculate n_{2DEG}=3.9×10^{13}cm^{-2}. However, earlier experimental results point on the difference with theoretical expectations [16]. In our simulations n_{2DEG}=2.7×10^{13}cm^{-2} provides the best agreement to measurement data.

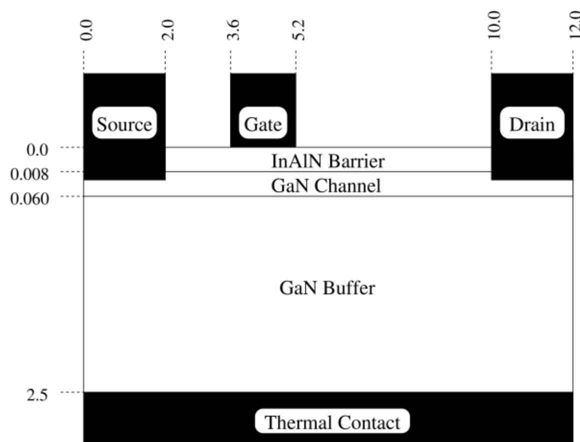

Fig.1: *Schematic view of investigated InAlN/GaN HEMT structure.*

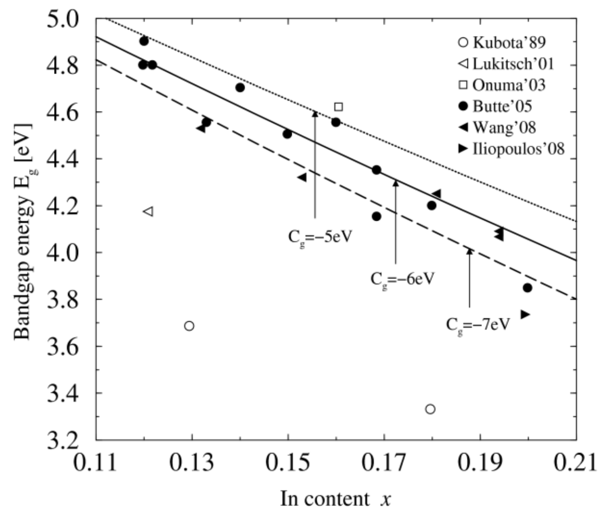

Fig.2: *Bandgap energy of $In_xAl_{1-x}N$ at 300K. Measured values (symbols) are compared to the model for different C_g (lines).*

4. Experimental and simulation results

In the following we present results of $In_{0.12}Al_{0.88}N$/GaN HEMT DC measurements and numerical simulations. *I-V* characteristics were measured using a highly-accurate, fully-automated semiconductor parameter analyzer Agilent 4155C with wolfram contact probes. The system includes four source monitor units (SMUs), two voltage monitor units (VMUs), and two voltage source units (VSUs). The transfer characteristics, shown in Fig.3, were measured for a V_{GS} sweep from –5V to 1V at V_{DS}=7V. The extracted threshold voltage is V_{th}~ –2.5V. To visualize the sub-threshold leakage current, Fig.4 shows the transfer characteristics and the extracted transconductance g_m also in logarithmic scale. Good agreement between simulation (lines) and experimental results (symbols) is obtained. Experimental and simulated output characteristics of Fig.5 are taken for a V_{DS} sweep from 0V to 15V; V_{GS} is stepped from –2V to 1V. The drop in the experimental output characteristics at the saturation is caused by self-heating which is not included in our simulations. The off-state breakdown (see Fig.6) was measured at V_{GS}=–5V with 10mA compliance. The drain voltage was ramped up from 0V with 1V steps. As Fig.6 indicates, the gate leakage current I_G is almost invariant to V_{DS}. On the other hand, the source-drain leakage current I_S increases steadily with V_{DS} and significantly overpasses I_G at V_{DS}=105V, when the hard breakdown occurs. This behavior strongly indicates that the breakdown event is triggered in the buffer layer of the device. In an earlier study, impact ionization has been accounted for the breakdown event [17], which is not considered in our simulations. Therefore, we calculate I_S only up to V_{DS}=105V in good agreement with our measured data. Fig.7 shows the simulated

two-dimensional electron concentration map of the studied HEMT in the pre-breakdown condition at V_{DS}=100V. A significant penetration of the space charge region into the GaN buffer and its extension towards the drain can be seen. Alternatively, for the same bias condition, Fig.8 shows the magnitude of the electric field in a cut along the HEMT channel which is compared with that at V_{DS}=10V. The peak electric field occurs at the drain side of the gate. A significant increase of its magnitude from ~1.5MV/cm at V_{DS}=10V up to ~6MV/cm at V_{DS}=100V is observed, which might cause impact ionization to occur [17].

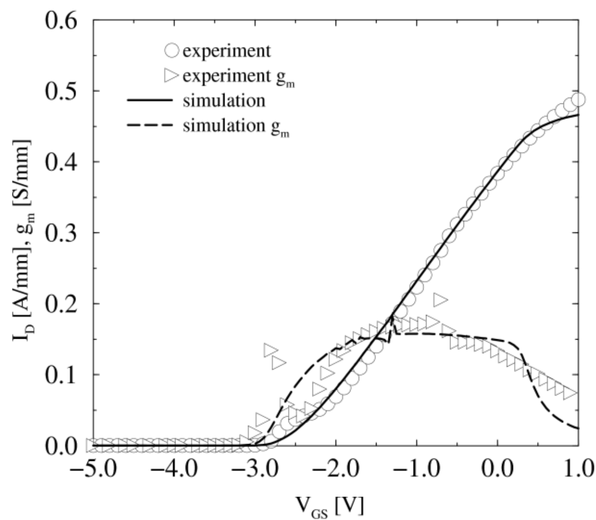

Fig.3: *Measured and simulated transfer characteristics and g_m at V_{DS}=7V.*

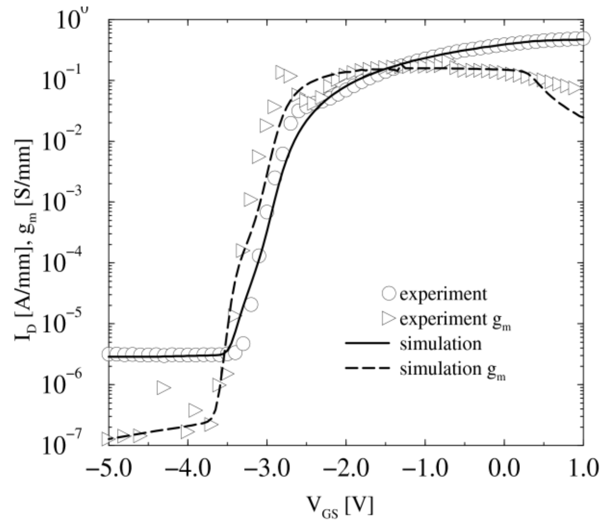

Fig.4: *Measured and simulated transfer characteristics and g_m at V_{DS}=7V.*

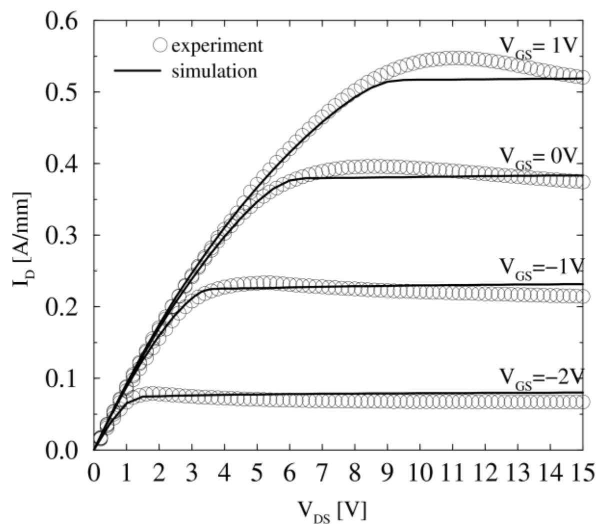

Fig.5: *Measured and simulated output characteristics.*

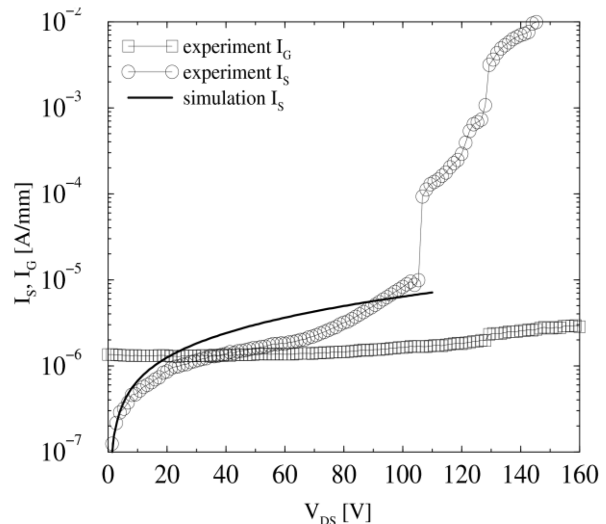

Fig.6: *Measured breakdown and simulated pre-breakdown characteristics at V_{GS}= –5V.*

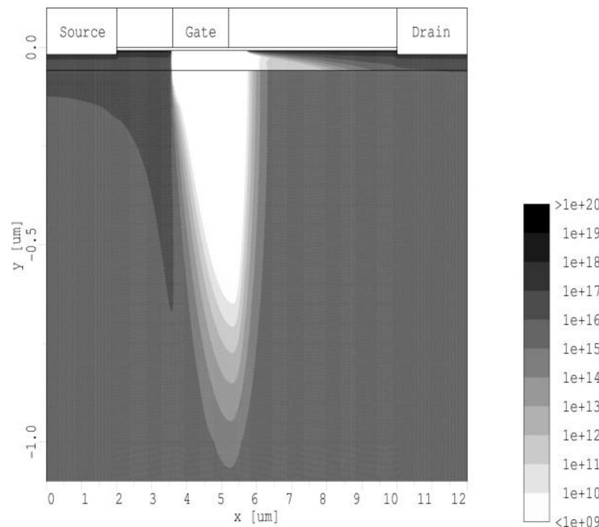

Fig.7: *Electron concentration [cm^{-3}] at V_{DS}=100V and V_{GS}= –5V.*

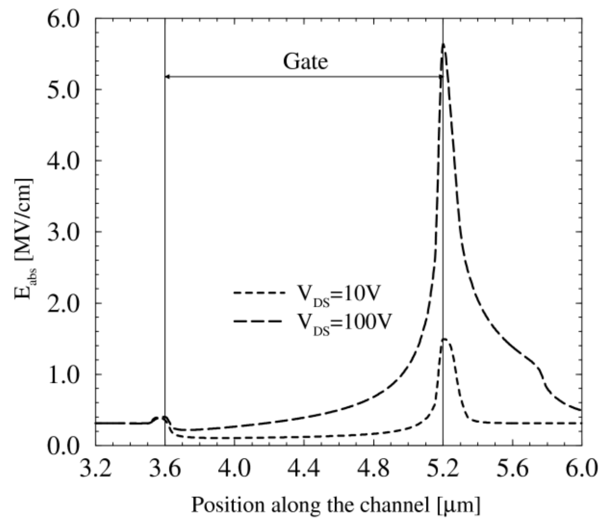

Fig.8: *Electric field along the channel for V_{DS}=*10V *and* 100V *at V_{GS}= –5V.*

5. Conclusion

Results from electrical measurements and two-dimensional numerical simulations of $In_{0.12}Al_{0.88}N$/GaN HEMT were presented. Very good agreement between experiment and simulation was obtained for both the transfer and the output characteristics using the hydrodynamic transport model. Results from the breakdown measurement and simulation of the HEMT at the pre-breakdown condition are also presented. Impact ionization in the GaN buffer is linked to the HEMT off-state breakdown.

Acknowledgement
This work was supported by the Austrian Science Funds FWF, START Project No.Y247-N13 and by grant VEGA 0866/11.

References:

[1] K. Takahashi, A. Yoshikawa, A. Sandhu: Wide Bandgap Semiconductors, Springer, New York (2007).
[2] S.M. Sze, K.K. Ng: Physics of Semiconductor Devices, Wiley, New Jersey (2007).
[3] R. Quay: Gallium Nitride Electronics, Springer, Berlin Heidelberg (2008).
[4] V. Palankovski, R. Quay: Analysis and Simulation of Heterostructure Devices, Springer, Wien New York (2004).
[5] S. Vitanov: Simulation of High Electron Mobility Transistors, Dissertation, TU Wien (2010). Available: http://www.iue.tuwien.ac.at/phd/vitanov
[6] H. Behmenburg, C. Giesen, R. Srnanek, J. Kovac, H. Kalisch, M. Heuken, R.H. Jansen: *J. Crystal Growth*, **316**, 42 (2011).
[7] S. Selberherr: Analysis and Simulation of Semiconductor Devices, Springer, Wien New York (1984).
[8] S. Vitanov, V. Palankovski, S. Maroldt, R. Quay: *Solid-State Electron.* **54**, 1105 (2010).
[9] S. Vitanov, V. Palankovski, S. Maroldt, R. Quay, S. Murad, T. Rödle, S. Selberherr: *IEEE Trans. Electron Devices,* **59**, 685 (2012).
[10] K. Kubota, Y. Kobayashi, K. Fujimoto: *J.Appl.Phys.,* **66**, 2984 (1989).

[11] M.J. Lukitsch, Y.V. Danylyuk, V.M. Naik, C. Huang, G.W. Auner, L. Rimai, R. Naik: *Appl.Phys.Lett.*, **30**, 632 (2001).
[12] T. Onuma, S.F. Chichibu, Y. Uchinuma, T. Sota, S. Yamaguchi, S. Kamiyama, H. Amano, I. Akasaki: *J.Appl.Phys.,* **94**, 2449 (2003).
[13] R. Butte, E. Feltin, J. Dorsaz, G. Christmann, J.-F. Carlin, N. Grandjean, M. Ilegems: *Jpn.J.Appl.Phys.*, **44**, 7207 (2005).
[14] K. Wang, R.W. Martin, D. Amabile, P.R. Edwards, S. Hernandez, E. Nogales, K.P. O'Donnell, K. Lorenz, E. Alves, V. Matias, A. Vantomme, D. Wolverson, I.M. Watson: *J.Appl.Phys.*, **103**, 073510 (2008).
[15] E. Iliopoulos, A. Adikimenakis, C. Giesen, M. Heuken, A. Georgakilas: *Appl.Phys.Lett.,* **92**, 191907 (2008).
[16] M. Gonschorek, J.-F. Carlin, E. Feltin, M.A. Py, N. Grandjean, V. Darakchieva, B. Monemar, M. Lorenz, G. Ram: *J.Appl.Phys.,* **103**, 093714 (2008).
[17] K. Kunihiro, K. Kasahara, Y. Takahashi, Y. Ohno: *IEEE Elec.Dev.Lett.,* **20**, 608 (1999).